ACS APPLIED MATERIALS & INTERFACES

Forum Article

www.acsami.org

Inkjet-Compatible Single-Component Polydiacetylene Precursors for Thermochromic Paper Sensors

Bora Yoon,[†] Hyora Shin,[†] Eun-Mi Kang,[†] Dae Won Cho,*[,‡] Kayeong Shin,[§] Hoeil Chung,[§] Chan Woo Lee,[⊥] and Jong-Man Kim*[,†,⊥]

[†]Department of Chemical Engineering, [§]Department of Chemistry, [⊥]Institute of Nanoscience and Technology, Hanyang University, Seoul 133-791, Korea

[‡]Department of Chemistry, Yeungnam University, Gyeongbuk 712-749, Korea

Supporting Information

ABSTRACT: Inkjet-printable diacetylene (DA) supramolecules, which can be dispersed in water without using additional surfactants, have been developed. The supramolecules are generated from DA monomers that contain bisurea groups, which are capable of forming hydrogen-bonding networks, and hydrophilic oligoethylene oxide moieties. Because of suitable size distribution and stability characteristics, the single DA component ink can be readily transferred to paper substrates by utilizing a common office inkjet printer. UV irradiation of the DA-printed paper results in generation of blue-colored polydiacetylene (PDA) images, which show reversible thermochromic transitions in specific temperature ranges. Inkjet-printed PDAs, in the format of a two-dimensional (2D) quick response (QR) code on a real parking ticket, serve as a dual anticounterfeiting system that combines easy decoding of the QR code and colorimetric PDA reversibility for validating the authenticity of the tickets. This single-component ink system has great potential for use in paper-based devices, temperature sensors, and anticounterfeiting barcodes.

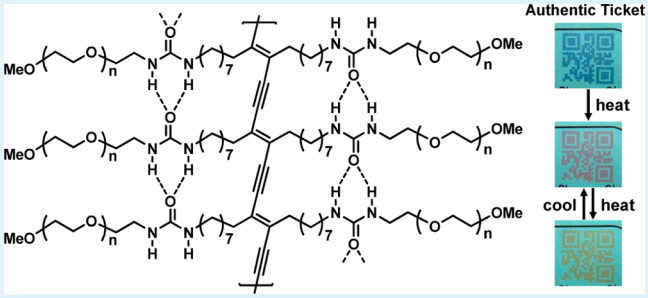

KEYWORDS: *polydiacetylene, inkjet printing, conjugated polymer, self-assembly, thermochromic sensor, paper sensor*

INTRODUCTION

Because of their readily available, lightweight, flexible, and disposable nature, paper-based functional devices have gained significant attention recently.[1−3] Various organic, inorganic, and biomaterials have been immobilized on paper substrates in applications ranging from electronics,[4−6] displays,[7−10] and solar cells[11] to sensors.[12−16] Among various techniques developed for the deposition of functional materials on paper, the inkjet printing method is of great interest because of its use in the facile generation of large-area image patterns in a high throughput manner, and low production costs and low waste materials associated with its employment.[17,18] The majority of inkjet printing of functional materials described to date, however, has involved hard surfaces such as glasses,[19] silicon wafers,[20] and flexible polymer films.[21] Inkjet printing of functional substances on paper substrates has been rarely used to date. In addition, thus far only a few reports have described the use of functional materials as inks that can be utilized in common office or household inkjet printers[22−24] in spite of the fact that inkjet devices developed for fabrication of specific scientific and industrial products have reached a high level of technical maturity. If such functional materials could be adapted to inkjet printing using a common office inkjet printer, it would be possible to utilize paper-based devices in both the scientific investigations and daily life applications.

From a materials perspective, polydiacetylenes (PDAs) are very promising substances because of their facile synthesis,[25−27] diverse morphologies,[28−30] as well as their stress-induced colorimetric and fluorometric transitions promoted by environmental stimulus such as heat,[31−34] ligand−receptor interactions,[35−40] magnetic field,[41] pH,[42,43] mechanical perturbations,[44] electrical current,[45] and organic solvents.[46,47] On the basis of the unique optical properties of PDAs, an inkjet-printable supramolecular system derived from a mixture of polymerizable amphiphilic diacetylenes (DAs) and surfactant molecules was recently developed.[48] In the device, a commercial black ink cartridge of a common office inkjet printer (HP Deskjet D2360) is loaded with an aqueous suspension of DA-surfactant complex. Printing of the suspension led to immobilization of DA supramolecules on an unmodified A4-sized paper. UV irradiation of the DA-printed paper was found to result in the generation of PDA images. The polymer immobilized on the paper substrate

Special Issue: Forum on Conjugated Polymer Materials for Sensing and Biomedical Applications

Received: December 31, 2012
Accepted: February 1, 2013
Published: March 7, 2013

   dx.doi.org/10.1021/am303300g | *ACS Appl. Mater. Interfaces* 2013, 5, 4527−4535

Scheme 1. Chemical Structures of Bolaamphiphilic Diacetylene Monomers for Single-Component Ink Systems

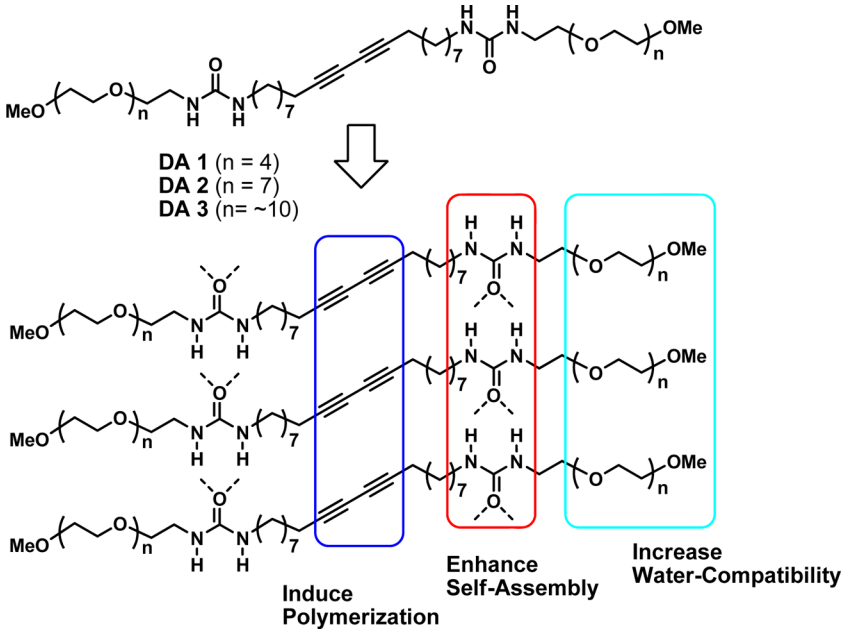

displayed typical chromic transitions in response to heat, pH, chemicals, and mechanical stimulations.

One critical disadvantage of using the reported DA ink formulation is that surfactant molecules (either ionic or nonionic) have to be used to increase the concentration of available DA monomers since direct printing of surfactant free DA monomers often results in the generation of poor PDA images. The two-component (DA and surfactant) ink system has an intrinsic phase separation problem, which could affect the long-term stability of the ink. To avoid the limitation associated with the two-component ink formulation, we have conducted studies to develop a single-component DA ink system. Introduction of hydrophilic functional groups, such as quaternary ammonium salt or sulfate groups, to the DA moieties enabled formation of water-soluble DA monomers. However, printing of an aqueous solution of the water-soluble DA monomers led to the inefficient photopolymerization after printing on a paper substrate. This observation indicates that DA monomers are not properly self-assembled during evaporation of water after the printing and immobilization steps.

Thus, an ideal single-component ink would have properly balanced self-assembly and hydrophilic properties. In addition, the DA ink should be compatible with the typical ink cartridge nozzle which is ca. 20 μm size.[22,48] With these goals in mind, we designed a single-component ink system that contains DA, bisurea and oligoethylene oxide moieties (Scheme 1). The DA functionality in the ink is responsible for the generation of PDA upon UV irradiation after printing. Second, because it is well-known that bisurea-substituted aliphatic chains form well organized self-assembled nanostructures, the bisurea motif was introduced to enhance supramolecular assembly of the monomer.[49−52] Lastly, the hydrophilic oligoethylene oxide moieties were expected to increase water compatibility of the monomer. If the three functional groups display ideal properties, they would comprise an inkjet-printable single component ink material. In order to explore this proposal, three single component ink systems containing the DA monomers DA **1**-DA **3** were prepared. In the monomers, the number of ethylene oxide units increase from 4 (DA **1**) to 7 (DA **2**) and to ca. 10 (DA **3**), which should lead to a corresponding enhancement in the hydrophilic property of the monomer. In the case of DA **3**, the exact number of the ethylene oxide group is not known precisely because the monomer is prepared from the commercially available poly(ethylene glycol) methyl ether only having an average molecular weight of 550.

EXPERIMENTAL SECTION

Materials and Instruments. 10,12-Docosadiyndioic acid (**4**) was purchased from GFS Chemicals, Ohio, USA. Pentaethylene glycol monomethyl ether (**6**) and octaethylene glycol monomethyl ether (**7**) were purchased from Tokyo Chemical Industry, Korea. Poly(ethylene glycol) methyl ether (**8**) and other common reagents were purchased from Aldrich, Korea. Scanning electron microscope (SEM) images were obtained using a JEOL (JSM-6330F) FE-SEM at an accelerating voltage of 15 kV. Each sample was coated with Pt for 30 s before analysis. Dynamic light scattering (DLS) data were collected using a Malvern ZEN3600. Raman spectra were collected with excitation at 785 nm laser using a Raman microscope (Kaiser Optical Systems). The absorption spectra measurements were recorded in absorbance measurement mode with a fiber optic spectrometer (Ocean Optics, USB 2000). The light from a tungsten halogen lamp was sent to the printed image via a fiber-optic probe. The reflected light from the image was acquired by the same probe and converted to the absorption spectra.

Synthesis of Diisocyanato-tethered Diacetylene 5. To a solution of diacetylene **4** (3.0 g, 8.3 mmol) in methylene chloride (100 mL) was added oxalyl chloride (3.15 g, 24.8 mmol) and then, the mixture solution was stirred at room temperature. After 30 min stirring, 0.3 mL of DMF was added dropwise and stirring was continued for 3 h. The resulting solution was filtered and concentrated in vacuo to give sticky residue. To this residue was added MeCN (100 mL) and NaN_3 (1.61 g, 24.8 mmol). The MeCN solution was stirred for 4 h at 50 °C. Filtration and concentration of the filtrate in vacuo gave the known diisocyanato-tethered diacetylene **5** (yield: 80%). ^{1}H NMR (300 MHz, $CDCl_3$, δ): 3.31 (t, J = 7.0 Hz, 4H), 2.24 (t, J = 6.9 Hz, 4H), 1.65−1.48 (m, 8H), 1.38−1.26 (m, 24H). ^{13}C NMR (300 MHz, $CDCl_3$, δ): 65.4, 43.0, 31.3, 29.0, 28.8, 28.7, 28.3, 26.5, 19.2; HRMS (ES, m/z): 357.2535 ($M+H^+$, $C_{22}H_{32}N_2O_2$ requires 357.2537).

Synthesis of Phthalimides 12−14. To a solution of the polyethyleneglycol methyl ether (5.0 g, 19.8 mmol of **6**, 7.6 g, 19.8

mmol of **7**, 10.9 g, 19.8 mmol of **8**) in THF (150 mL) was added triethylamine (8.3 mL, 59.4 mmol). After 30 min stirring at room temperature, MsCl (3.1 mL, 39.6 mmol) was added dropwise to the solution and the resulting solution was stirred for 4 h at the same temperature. Extraction with methylene chloride, followed drying and evaporation in vacuo of the extract gave the desired mesylate (**9**-**11**). To an MeCN (150 mL) of mesylate was added K-phthalimide salt (5.5 g, 29.7 mmol for **9**-**11**) and the resulting solution was stirred at reflux (over 90 °C) for 5 h. After removing excess K-phthalimide by filtration, the MeCN solution was concentrated in vacuo to give a residue, which was extracted with methylene chloride. The extract was dried and concentrated in vacuo to yield the phthalimide derivative (yield: 90% of **12**, 85% of **13**, 84% of **14**).

12: ^{1}H NMR (300 MHz, $CDCl_3$, δ): 7.88−7.84 (m, 2H), 7.75−7.72 (m, 2H), 3.91 (t, J = 6.0 Hz, 2H), 3.74 (t, J = 6.0 Hz, 2H), 3.66−3.53 (m, 16H), 3.39 (s, 3H); ^{13}C NMR (300 MHz, $CDCl_3$, δ): 168.2, 134.1, 132.1, 123.9, 123.8, 72.1, 70.4, 70.2, 68.0, 59.1, 37.2; HRMS (ES, m/z): 404.1681 ($M+Na^+$, $C_{19}H_{27}NO_7Na$ requires 404.1680).

13: ^{1}H NMR (300 MHz, $CDCl_3$, δ): 7.88−7.84 (m, 2H), 7.75−7.73 (m, 2H), 3.92 (t, J = 6.0 Hz, 2H), 3.74 (t, J = 6.0 Hz, 2H), 3.67−3.53 (m, 28H), 3.38 (s, 3H). ^{13}C NMR (300 MHz, $CDCl_3$, δ): 168.4, 134.4, 134.0, 132.8, 132.2, 123.7, 123.4, 72.0, 70.7, 70.6, 70.2, 68.0, 59.2, 37.3. HRMS (ES, m/z): 536.2465 ($M+Na^+$, $C_{25}H_{39}NO_{10}Na$ requires 536.2466).

14: ^{1}H NMR (300 MHz, $CDCl_3$, δ): 7.87−7.84 (m, 2H), 7.76−7.73 (m, 2H), 3.91 (t, J = 6.0 Hz, 2H), 3.74 (t, J = 6.0 Hz, 2H), 3.67−3.53 (m, ∼40H), 3.38 (s, 3H); ^{13}C NMR (300 MHz, DMSO-d_6, δ): 169.3, 135.8, 134.3, 132.6, 131.6, 130.8, 124.2, 123.0, 79.0, 71.1, 69.8, 58.1, 42.6.

Synthesis of Aminoethyl(polyethylene glycol) Methylethers 15−17. To a solution of each phthalimide (3.0 g, 7.86 mmol of **12**, 4.0 g, 7.86 mmol of **13**, 5.3 g, 7.76 mmol of **14**) in ethanol:THF (1: 1 v/v, 160 mL) was added hydrazine monohydrate (2.0 g, 40 mmol). The solution was stirred at reflux (90 °C) for 10 h. Filtration followed by evaporation in vacuo of the filtrate gave a residue that was extracted with methylene chloride and sat. $NaHCO_3$. The extract was dried and concentrated in vacuo to give the amine derivative (88% of **15**, 84% of **16**, 84% of **17**).

15: ^{1}H NMR (300 MHz, $CDCl_3$, δ): 3.64−3.61 (m, 16H), 3.59−3.51 (m, 4H), 3.39 (s, 3H); ^{13}C NMR (300 MHz, $CDCl_3$, δ): 72.8, 72.7, 72.0, 70.7, 70.6, 70.3, 70.1, 61.7, 59.1, 49.3, 37.8, 29.8.

16: ^{1}H NMR (300 MHz, $CDCl_3$, δ): 3.66−3.62 (m, 28H), 3.59−3.51 (m, 4H), 3.38 (s, 3H); ^{13}C NMR (300 MHz, $CDCl_3$, δ): 72.9, 72.8, 72.0, 70.7, 70.6, 70.3, 61.8, 59.1, 42.0, 32.0, 30.2, 29.8.

17: ^{1}H NMR (300 MHz, $CDCl_3$, δ): 3.67−3.61 (m, ∼40H), 3.60−3.56 (m, 4H), 3.38 (s, 3H); ^{13}C NMR (300 MHz, $CDCl_3$, δ): 72.5, 71.7, 70.4, 69.0, 61.4, 58.9, 40.8.

Synthesis of Bis(polyethyleneglycidylurea)-tethered Diacetylenes DA 1−3. To independent solutions of diacetylene **5** (0.5 g, 1.25 mmol) and triethylamine (0.52 mL, 3.76 mmol) in chloroform (15 mL) were added the amino methylethers (0.94 g, 3.76 mmol of **15**, 1.44 g, 3.76 mmol of **16**, 2.1 g, 3.76 mmol of **17**). The mixtures were stirred at reflux 80 °C for 10 h. Extraction of each solution with chloroform and 1 *N* NaOH (x 2 times) gave organic layers that were dried and concentrated in vacuo to give the final products (yield: 77% of DA **1**, 80% of DA **2**, 70% of DA **3**), respectively.

DA **1**: ^{1}H NMR (300 MHz, $CDCl_3$, δ): 5.28−5.23 (m, 2H), 5.08−5.02 (m, 2H), 3.66−3.51 (m, 36H), 3.38−3.34 (m, 10H), 3.14 (q, J = 6.6 Hz, 4H), 2.22 (t, J = 6.6 Hz, 4H), 1.53−1.46 (m, 8H), 1.40−1.22 (m, 16H); ^{13}C NMR (300 MHz, $CDCl_3$, δ): 159.1, 71.9, 70.9, 70.7, 70.6, 70.5, 70.1, 65.5, 59.1, 41.1, 40.4, 40.3, 36.2, 29.4, 29.1, 28.9, 28.3, 27.1, 19.2; HRMS (ES, m/z): 430.3036 ($((M+2H)^{2+}/2$, $C_{22}H_{43}N_2O_6$ requires 430.3037).

DA **2**: ^{1}H NMR (300 MHz, $CDCl_3$, δ): 5.26−5.22 (m, 2H), 5.04−5.00 (m, 2H), 3.63−3.50 (m, 60H), 3.36−3.32 (m, 10H), 3.10 (q, J = 6.9 Hz, 4H), 2.21 (t, J = 6.6 Hz, 4H), 1.53−1.46 (m, 8H), 1.40−1.20 (m, 16H); ^{13}C NMR (300 MHz, $CDCl_3$, δ): 158.9, 72.0, 70.8, 70.6, 70.5, 70.4, 70.3, 70.1, 65.4, 59.1, 41.2, 41.0, 40.3, 40.2, 36.3, 30.5, 30.4, 29.8, 29.3, 29.2, 29.1, 29.0, 28.9, 28.8, 28.4, 28.3, 27.0, 26.9, 19.2; HRMS (ES, m/z): 562.3823 ($((M+2H)^{2+}/2$, $C_{28}H_{55}N_2O_9$ requires 562.3824).

DA **3**: ^{1}H NMR (300 MHz, $CDCl_3$, δ): 5.35−5.26 (m, 2H), 5.04−5.00 (m, 2H), 3.66−3.51 (m, ∼84H), 3.36−3.30 (m, 10H), 3.11 (q, J = 6.4 Hz, 4H), 2.21 (t, J = 6.9 Hz, 4H), 1.51−1.43 (m, 8H), 1.42−1.22 (m, 16H); ^{13}C NMR (300 MHz, $CDCl_3$, δ): 158.9, 72.0, 70.8, 70.6, 70.5, 70.4, 70.3, 70.1, 65.1, 59.2, 41.0, 40.2, 36.3, 30.2, 29.9, 29.4, 29.3, 29.2, 29.1, 29.0, 28.9, 28.4, 27.0, 19.2.

Preparation of Single-Component Ink Solutions. A solution of DA **1** (7.7 mg) in DMSO (0.2 mL) was injected into deionized water (3 mL) to yield a total monomer concentration of 3 mM. The resulting suspension was sonicated for 10 min at room temperature. DA **2** and DA **3** were dissolved in deionized water to yield a total monomer concentration of 50 mM. The resulting suspensions were sonicated for 10 min in an ice bath. Following sonication, the solutions were kept in the refrigerator. Black ink solution from a conventional inkjet office printer (HP Deskjet D2360) cartridge was removed, and the cartridge was thoroughly washed with ethanol, water and dried with a N_2 blowing. The diacetylene ink (0.2 mL), prepared as described above was then loaded in the cartridge.

RESULTS AND DISCUSSION

Preparation of Diacetylene Monomers. The initial phase of the current investigation focused on the synthesis of polyethyleneglycidylurea-tethered DA **1**−**3**. Convergent synthetic routes to these substances begin with the preparation of the diisocyanate group-tethered DA **5** and aminoethyl-(polyethylene glycol) methylethers **15**-**17**[53] (Scheme 2).

Scheme 2. Synthesis of Diacetylene Monomers DA 1−DA 3

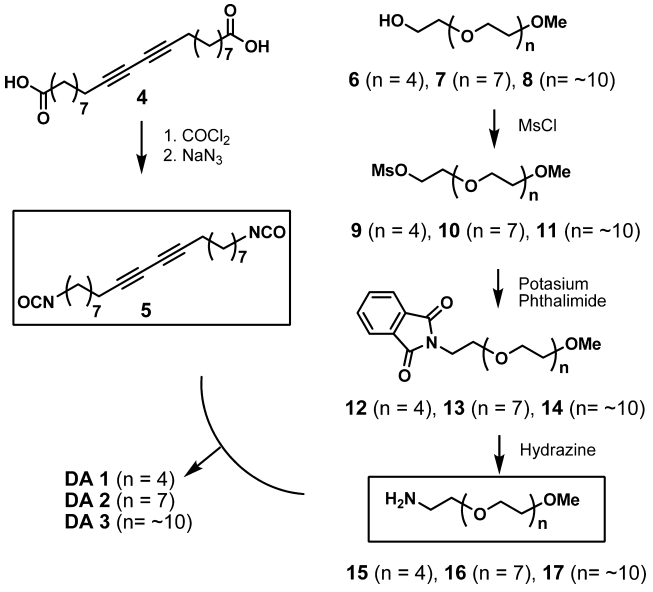

Reaction of DA **4** with oxalyl chloride affords acid chloride, which is easily transformed to diisocyanate group-tethered DA **5** by treatment of sodium azide. On the other hand, preparation of amines **15**−**17** starts with reactions of polyethyleneglycol methylethers **6**−**8** and methanesulfonyl chloride (MsCl) followed by deprotection of phthalimide moieties to give amines **15**−**17**. The final DA monomers, DA **1**−**3** are prepared in high yields (70−80%) by condensation of **5** with −-**17**, respectively, in the presence of triethylamine.

Single-Component Ink System. To prepare single-component inks, the DA **1**−**3** monomers were dissolved in deionized water to yield a total monomer concentration of 50 mM. It was difficult to disperse DA **1** in water because of its

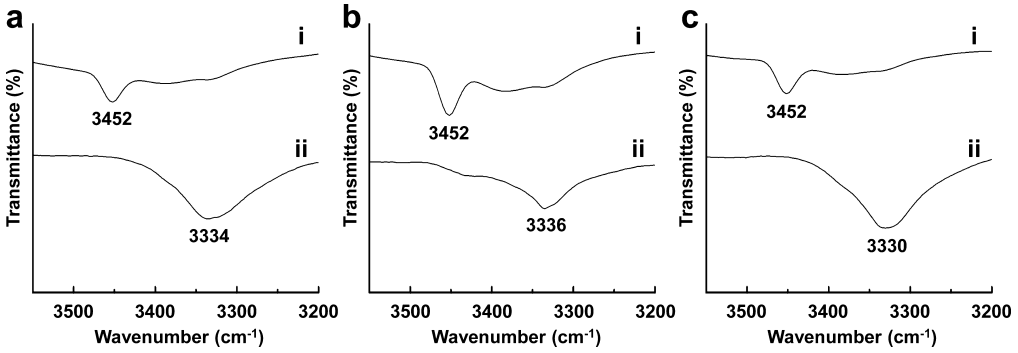

Figure 1. FTIR spectra of (a) DA **1**, (b) DA **2**, and (c) DA **3**: (i) in $CHCl_3$, (ii) a KBr pellet prepared by freeze-drying of a corresponding PDA aqueous solution.

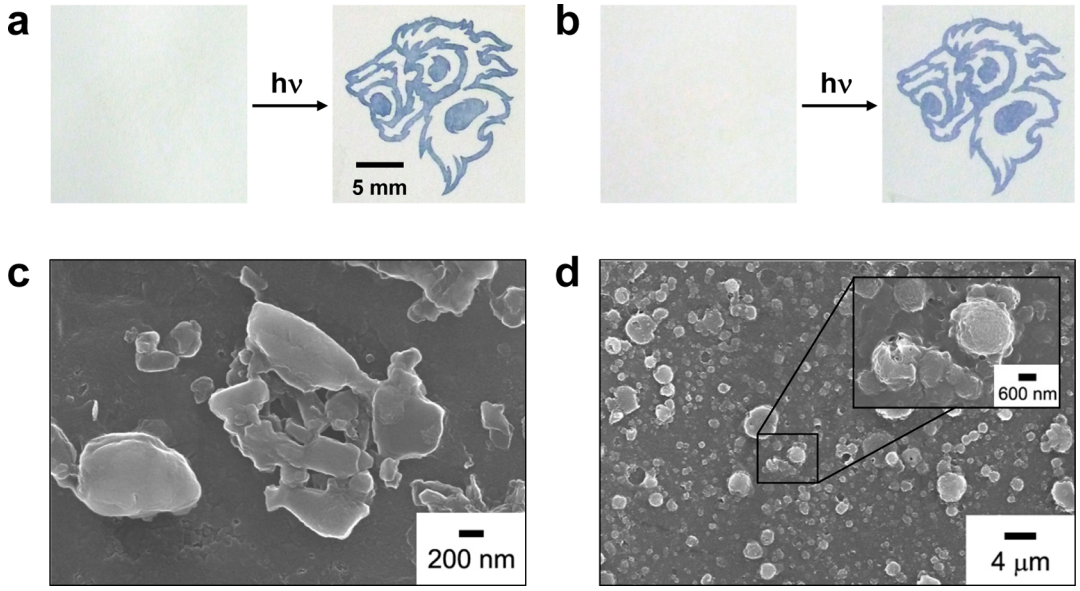

Figure 2. Photographs of printed images on an unmodified paper substrate using PDA ink solutions derived from (a) DA **2** and (b) DA **3** before (left) and after (right) 254 nm UV irradiation (1 mW cm^{-2}, 5 min). SEM images of PDA fabricated on photopaper using PDA ink solutions derived from (c) DA **2** and (d) DA **3** after 254 nm UV irradiation (1 mW cm^{-2}, 5 min).

severe aggregation tendency and low water affinity caused by the presence a relatively short oligoethylene oxide unit. Thus, a DA **1** suspension could only be obtained by employing the conventional injection method with a maximum concentration of about 3 mM (see Experimental Section). Irradiation of the suspension with 254 nm light resulted in a blue-colored solution (see Figure S1a in the Supporting Information). In contrast, DA **2** and DA **3** were found to form well-dispersed self-assembled supramolecules in aqueous solution with concentrations that are almost ten times higher than the maximum achievable concentration of vesicles derived from oligoethylene oxide modified DAs that we previously reported (see Figure S1b, S1c in the Supporting Information).[54] Thus, the hydrophilic oligoethylene oxide moieties and bisurea groups in DA **2** and DA **3** allow good water compatibility as well as polymerizable supramolecular assembly of the monomers in aqueous solution. Both pale yellow solutions formed from DA **2** and DA **3** were transformed to intense blue-colored PDAs upon 254 nm UV irradiation for 3 min.

In the next phase of the investigation, we determined that hydrogen-bonding interactions involving the bisurea groups take place in the self-assembled PDA supramolecules by using Fourier transform infrared (FTIR) analysis. To monitor the intermolecular hydrogen-bonding of the bisurea groups before and after self-assembly, solutions in $CHCl_3$ and KBr pellets (obtained by freeze-drying of DA supramolecules in aqueous solution) of the monomers were prepared. Depicted in Figure 1a are the FTIR spectra of DA **1** in $CHCl_3$ (i) and a KBr pellet of the corresponding self-assembled DA supramolecules after freeze-drying (ii). The position of absorption band for N−H stretching in $CHCl_3$ (3452 cm^{-1}) is shifted to a lower wavenumber of 3334 cm^{-1} and broadened after self-assembly, an observation that demonstrates the formation of hydrogen-bonds between the bisurea groups.[51,52,55] The free urea N−H stretching bands of DA **2** (Figure 1b, i) and DA **3** (Figure 1c, i) are also clearly shifted to ones corresponding to hydrogen-bonded structures at 3336 (Figure 1b, ii) and 3330 cm^{-1} (Figure 1c, ii), respectively, in the self-assembled solid state (KBr pellet). In addition, the presence of two characteristic absorption bands, including one for C═O stretching (amide I, $\nu_{CO} \approx 1615$ cm^{-1}) and a combination for N−H bending and C−N stretching vibrations (amide II, $\delta_{NH} + \nu_{CN} \approx 1575$ cm^{-1}), of KBr pellets indicates that the bisurea groups of self-assembled DA supramolecules are involved in hydrogen-bonding interactions (see Figure S2 in the Supporting Information).[51]

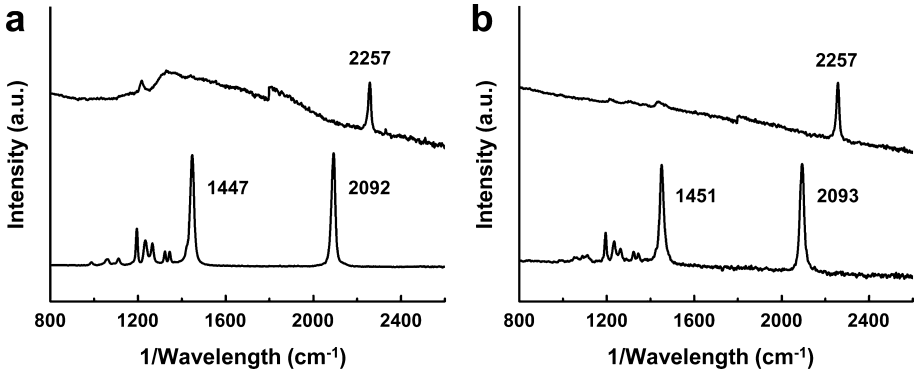

Figure 3. Raman spectra of (a) DA **2** and (b) DA **3** in chloroform (top) and printed on an unmodified paper substrate following polymerization (254 nm, 1 mW cm^{-2}, 5 min) (bottom).

One of the most important requirements of a single-component DA ink solution for inkjet printing is that the supramoleculary assembled DA monomers be sufficiently small to pass through a cartridge nozzle with a pore size of ca. 20 μm diameter. To explore this feature, size distributions of ink solutions were determined by using the dynamic light scattering (DLS) method. The ink solution derived from DA **1** was unsuitable for this purpose owing to the fact that it formed large aggregates of sized more than 8 μm with a high polydispersity (data not shown). This finding indicates that even though DA **1** seems to form self-assembled supramolecules in aqueous solution (Figure 1a), in reality it produces irregular microsized DA **1** aggregates in the ink solution. On the other hand, ink solutions derived from DA **2** and DA **3**, despite their high concentrations compared to DA **1**, were found to display uniform size distributions with mean diameters of 780 and 304 nm, respectively (see Figure S3 in the Supporting Information).

To test the suitability of the solutions for inkjet printing, we used a computer-controlled conventional thermal inkjet office printer (HP Deskjet D2360) with a black cartridge thoroughly washed with ethanol and water. The cartridge was filled with a single component ink solution that was then printed on an unmodified paper substrate. In the case of DA **1**, printed images could not be produced owing to its insufficient water compatibility and aggregation tendency. In contrast, as expected based on the DLS results, ink solutions derived from DA **2** and DA **3** did not cause nozzle clogging of the cartridge and printing on the paper was carried out smoothly. After printing each ink, images were not visible because the DA monomers do not absorb visible light. However, UV irradiation of the printed image initiated polymerization of the DA monomers and resulted in the formation of a blue-colored PDA image patterns (Figure 2a, b). This observation confirms that DA monomers are sufficiently well aligned and closely packed after printing for polymerization to occur. In images c and d in Figure 2 are displayed scanning electron microscopic (SEM) images of PDAs derived from DA **2** and DA **3**, respectively, printed on a photopaper. Photopaper (Kodat Premium Glossy Photo Paper, 210 μm) with a smooth surface was used instead of the unmodified paper having the complicated surface morphology for the SEM observation. Inspection of both images shows that the amorphous aggregates are small enough to pass through a cartridge nozzle of 20 μm size and the observation of PDA particles evidence the fact that immobilization on the photopaper has taken place.

To verify the formation of PDAs printed on the paper substrate, we used Raman spectroscopy to probe the changes in diacetylenic units before and after polymerization. As seen by viewing the spectra shown in Figure 3a, the acetylenic stretching band of monomeric DA **2** in chloroform solution (top) occurs at 2257 cm^{-1}. After UV irradiation of the printed image of DA **2**-derived ink solution, the acetylenic stretching band of DA **2** disappears and two bands, associated with conjugated alkyne−alkene structures of blue-phase PDA, appear at 2092 (C≡C) and 1447 cm^{-1} (C═C) (Figure 3a, bottom).[56] In a similar manner, the Raman spectrum of a chloroform solution of DA **3** contains a monomeric acetylene band of 2257 cm^{-1} (Figure 3b, top). Upon irradiation of the DA **3**-derived ink printed paper, the typical conjugated blue-phase PDA Raman bands appears at 2093 (C≡C) and 1451 cm^{-1} (C═C) with in concert with disappearance of the monomeric band (Figure 3b, bottom). The spectroscopic results provide evidence that most of monomers in the both DA **2** and DA **3** are transformed to PDA by UV irradiation.

In terms of stability, ink solutions containing DA **2** and DA **3** have a tendency to form precipitates after prolonged storage (>1 month). Although this tendency might be associated with their high concentrations, shaking of the containers is sufficient to redisperse the monomers and generate inks that are useful for inkjet printing. We have also found that in comparison to the DA **2**-derived ink solution, printing using a DA **3**-derived ink solution that had been stored in a refrigerator for 1 year gives a high quality printed image (see Figure S4 in the Supporting Information). In addition, the image quality obtained from the DA **3**-derived ink stored for 1 year was as good as that obtained using freshly prepared ink.

Thermchromism of PDA Images on Paper Substrates. The thermochromic reversibility of PDAs has been widely investigated with regard to the structures of DA monomers.[26,57] In a recent publication, we described PDAs that when printed on paper display a reversible thermochromic transition.[48] To improve the reversible thermochromism of PDAs, we have modified DA monomers so that they have the capability of forming strong hydrogen-bonding networks and aromatic interactions in headgroups. On the basis of the results of the previous study, we anticipated that the bisurea group containing monomers DA **2** and DA **3**, which have the potential of displaying sufficiently strong hydrogen-bonding interactions would produce reversible thermochromic PDAs even on a paper substrate. In order to test this proposal, the bisurea containing PDA-patterned paper was placed on a temperature-controlled hot plate and the color was monitored at different

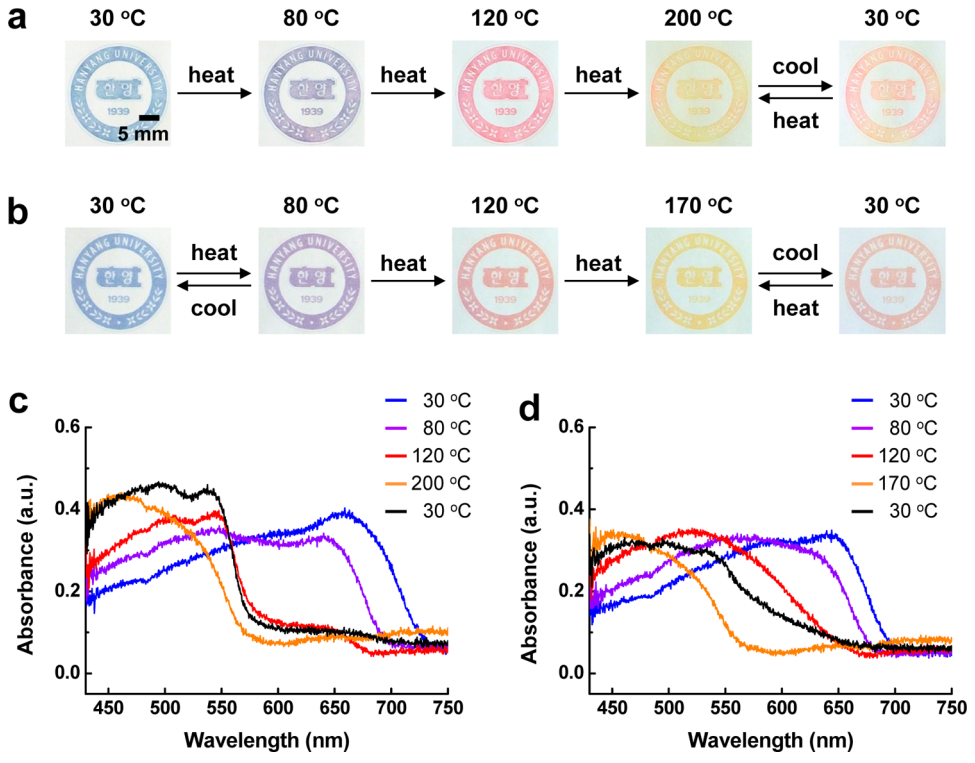

Figure 4. Photographs of printed images of (a) DA **2**-derived PDAs and (b) DA **3**-derived PDAs on an unmodified paper substrate upon thermal stimulation. UV−vis absorption spectra of (c) DA **2**-derived PDAs and (d) DA **3**-derived PDAs printed on an unmodified paper substrate as a function of the temperature. Black lines in each spectrum are the final phase involving cooling to 30 °C.

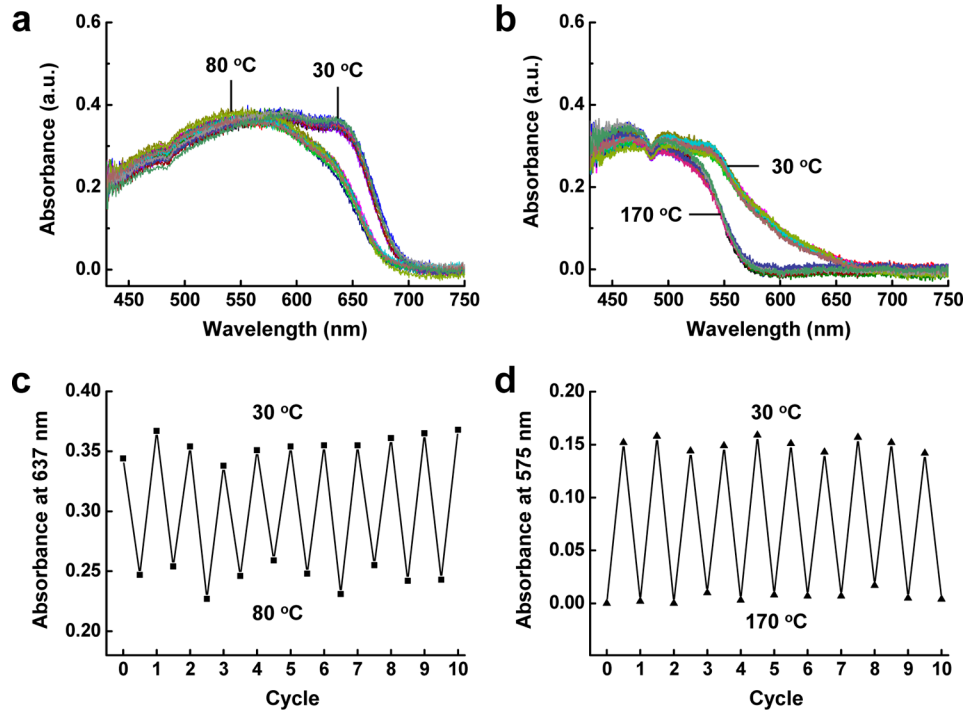

Figure 5. (a, b) UV−vis absorption spectra of DA **3**-derived PDAs printed on an unmodified paper substrate upon thermal cycle. Plots of (c) absorbance at 637 nm between 30 and 80 °C, and (d) absorbance at 575 nm between 30 and 170 °C as a function of the thermal cycle.

temperatures. In Figure 4a is displayed the picture of a printed image of DA **2**-derived PDAs on paper during the heating process. The color of the PDA changed from blue to purple at 80 °C and then to red at 120 °C. Upon heating to 200 °C, both yellow and yellowish red-colored PDAs were observed in the same pattern. Further heating above 200 °C generated an entirely yellow-colored polymer but the white-colored paper substrate gradually turned brown at this high temperature, thus giving rise to an unclear yellow image. Upon cooling to 30 °C, the yellowish PDA pattern undergoes a reversible color

dx.doi.org/10.1021/am303300g | ACS Appl. Mater. Interfaces 2013, 5, 4527−4535

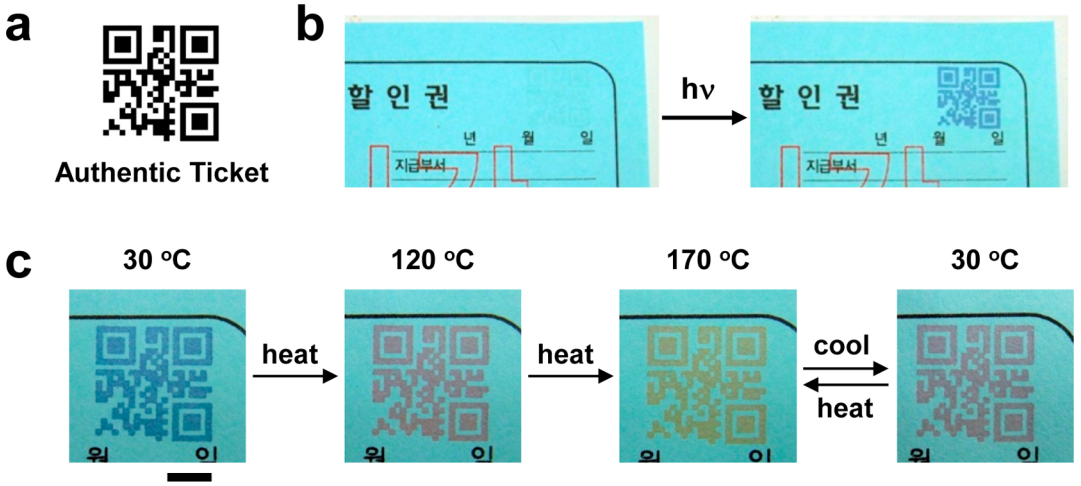

Figure 6. (a) Original image of QR code encoded with the word "Authentic Ticket". (b, c) Photographs of printed QR codes on a parking ticket using (b) ink solution derived from DA **3** as printed (left), after 254 nm UV irradiation (1 mW cm^{-2}, 5 min) (right), and (c) heat treatment (scale bar: 4 mm).

transition from yellow to red. Interestingly, the DA **3**-derived PDA, the image of which is shown in Figure 4b, was found to display a completely reversible thermochromism in two temperature ranges, from 30 to 80 °C and from 170 to 30 °C. The blue-colored PDA becomes purple at 80 °C and it reverts back to the initial blue color upon cooling to 30 °C. Once it is heated over 80 °C, the PDA pattern undergoes an irreversible color transition to red at 120 °C and then to yellow at 170 °C. However, upon cooling to 30 °C, the DA **3**-derived PDA shows complete colorimetric reversibility between yellow and red.

The excellent thermochromic reversibility of DA **3**-derived PDA is presumably a consequence of a proper balance between the water compatibility of the long hydrophilic oligoethylene oxide moieties and the hydrogen-bonding ability of the bisurea group. In addition, DA **3** is found to be better dispersed in deionized water with smaller mean diameter (304 nm) than DA **2** (780 nm). In panels c and d in Figure 4 are displayed absorption spectra of printed PDAs derived from DA **2** and DA **3** as a function of temperature. Both DA **2** and DA **3**-derived PDAs display gradual blue shifts in their absorption spectra as the temperature increases. In accord with the colorimetric changes displayed in panels a and b in Figure 4, the absorption maxima shift back to red-phase positions (black line in spectrum) upon cooling to 30 °C. The full temperature range photographs and spectroscopic results of printed PDAs derived from DA **2** and DA **3** are provided in Figures S5 and S6 in the Supporting Information.

The reversible thermochromism of DA **3**-derived PDA in two temperature ranges, from 30 to 80 °C and from 170 to 30 °C was also monitored by using absorption spectroscopy (Figure 5a, b). As expected, the DA **3**-derived PDA displays complete colorimetric reversibility between blue and purple (Figure 5a) as well as between yellow and red (Figure 5b). The colorimetric reversibility of the PDA-derived from DA **3** is also revealed in the plot of absorbances at 637 nm (Figure 5c) and 575 nm (Figure 5d) during the thermal cycle. In addition, the stability of the printed images was demonstrated by observing that color is not lost during repeating the thermal cycle (>100 times).

The final phase of the current investigation focused on the application of the colorimetrically reversible DA **3**-derived PDA to printing a parking ticket barcode for authentication purposes. Among various barcode systems, a two-dimensional (2D) quick response (QR) code is of great interest because of its ability to provide a high information density with error correction features and to encode all types of data such as symbols, binary codes and multimedia data, which can be easily decoded by using a QR code reader application of a smartphone.[58−61] To demonstrate the anticounterfeiting and authentication abilities of DA **3**-derived PDA, a QR code encoded with the word "Authentic Ticket" (Figure 6a) was printed on a real parking ticket. As seen by inspecting the images in Figure 6b, UV irradiation (1 mW cm^{-2}, 5 min) of the printed ticket generates the blue-colored QR code with a resolution that is similar to that of original pattern comprised of submillimeter-sized black and white dots. The movie clip provided in the Supporting Information clearly demonstrates the decoding process of QR-coded parking ticket by utilizing a QR code reader application (Bakodo, Bakodo Inc.) of a smartphone (iPhone 4S, Apple Inc.). Although the inkjet-printed monomeric QR code on a parking ticket was found to be polymerized under room light within a month, we have found that blue-phase QR code was stable and decodable after storage under ambient conditions for over 4 months (see Figure S7 in the Supporting Information). As expected, the blue-colored QR code undergoes a colorimetric transition from blue to red at 120 °C and then to yellow at 170 °C, processes which can be reversed (yellow-to-red) by cooling the ticket to room temperature (Figure 6c). In this case, the purple-colored QR code formed at about 80 °C is difficult to distinguish owing to the blue background color of the ticket. As a result, the process enables construction of a dual anticounterfeiting system for a parking ticket combined with the easily decodable QR code and the colorimetrically reversible PDA as a visible security feature.

CONCLUSIONS

The studies described above have led to the development of a single component ink system for thermochromic conjugated polymers. Introduction of oligoethylene oxide moieties and bisurea groups into DA monomers gives rise to a highly concentrated self-assembled PDA supramolecules in an aqueous solution. The hydrogen-bonding interaction between bisurea groups of the polymerized ink solution was found to

dx.doi.org/10.1021/am303300g | ACS Appl. Mater. Interfaces 2013, 5, 4527−4535

increase as the number of ethylene oxide unit increases without disturbing the closely packed self-assembled structures. The ink solution was readily transferred to a paper substrate by utilizing a common office inkjet printer. UV-induced photopolymerization of the DA-printed paper resulted in blue-colored conjugated PDAs, which displayed completely reversible thermochromic transitions in particular temperature ranges. In addition, a QR code printed with colorimetrically reversible PDAs on a real parking ticket serves as a dual anticounterfeiting system for authentic identification of tickets. It is believed that the new method, utilizing direct inkjet printing of thermochromic conjugated polymers, will have potential applications to paper-based devices, temperature sensors, and anticounterfeiting barcode systems.

■ ASSOCIATED CONTENT

Supporting Information

Photographs of polydiacetylene ink solutions, FTIR spectra, dynamic light scattering analysis, stability of ink solutions, and UV−vis absorption spectra of polydiacetylenes printed on an unmodified paper substrate as a function of a temperature; video clip demonstrating the decoding process of a QR-coded parking ticket. This material is available free of charge via the Internet at http://pubs.acs.org/.

■ AUTHOR INFORMATION

Corresponding Author

*E-mail: jmk@hanyang.ac.kr (J.-M.K.); dwcho00@yu.ac.kr (D.W.C.).

Notes

The authors declare no competing financial interest.

■ ACKNOWLEDGMENTS

The authors gratefully thank the National Research Foundation of Korea (NRF) for financial support through Basic Science Research Program (20120006251 and 2012R1A6A1029029), Nano Material Technology Development Program (2012035286), and Center for Next Generation Dye-Sensitized Solar Cells (20120000593). This work was also supported by Genic Co (2012-000-0000-0760).

■ REFERENCES

(1) Mazzeo, A. D.; Kalb, W. B.; Chan, L.; Killian, M. G.; Bloch, J.-F.; Mazzeo, B. A.; Whitesides, G. M. *Adv. Mater.* **2012**, *24*, 2850−2856.
(2) Tobjörk, D.; Österbacka, R. *Adv. Mater.* **2011**, *23*, 1935−1961.
(3) Nyholm, L.; Nyström, G.; Mihranyan, A.; Strømme, M. *Adv. Mater.* **2011**, *23*, 3751−3769.
(4) Zschieschang, U.; Yamamoto, T.; Takimiya, K.; Kuwabara, H.; Ikeda, M.; Sekitani, T.; Someya, T.; Klauk, H. *Adv. Mater.* **2011**, *23*, 654−658.
(5) Russo, A.; Ahn, B. Y.; Adams, J. J.; Duoss, E. B.; Bernhard, J. T.; Lewis, J. A. *Adv. Mater.* **2011**, *23*, 3426−3430.
(6) Siegel, A. C.; Phillips, S. T.; Dickey, M. D.; Lu, N.; Suo, Z.; Whitesides, G. M. *Adv. Funct. Mater.* **2010**, *20*, 28−35.
(7) Kim, D. Y.; Steckl, A. J. *ACS Appl. Mater. Interfaces* **2010**, *2*, 3318−3323.
(8) Tehrani, P.; Hennerdal, L.-O.; Dyer, A. L.; Reynolds, J. R.; Berggren, M. *J. Mater. Chem.* **2009**, *19*, 1799−1802.
(9) Hennerdal, L.-O.; Berggren, M. *Appl. Phys. Lett.* **2011**, *99*, 183303.
(10) Siegel, A. C.; Phillips, S. T.; Wiley, B. J.; Whitesides, G. M. *Lab Chip* **2009**, *9*, 2775−2781.
(11) Fan, K.; Peng, T.; Chen, J.; Zhang, X.; Li, R. *J. Mater. Chem.* **2012**, *22*, 16121−16126.
(12) Mirica, K. A.; Weis, J. G.; Schnorr, J. M.; Esser, B.; Swager, T. M. *Angew. Chem., Int. Ed.* **2012**, *51*, 10740−10745.
(13) Lee, J.; Seo, S.; Kim, J. *Adv. Funct. Mater.* **2012**, *22*, 1632−1638.
(14) Cheng, C.-M.; Martinez, A. W.; Gong, J.; Mace, C. R.; Phillips, S. T.; Carrilho, E.; Mirica, K. A.; Whitesides, G. M. *Angew. Chem., Int. Ed.* **2010**, *49*, 4771−4774.
(15) Xu, M.; Bunes, B. R.; Zang, L. *ACS Appl. Mater. Interfaces* **2011**, *3*, 642−647.
(16) Eaidkong, T.; Mungkarndee, R.; Phollookin, C.; Tumcharern, G.; Sukwattanasinitt, M.; Wacharasindhu, S. *J. Mater. Chem.* **2012**, *22*, 5970−5977.
(17) deGans, B. J.; Duineveld, P. C.; Schubert, U. S. *Adv. Mater.* **2004**, *16*, 203−213.
(18) Calvert, P. *Chem. Mater.* **2001**, *13*, 3299−3305.
(19) Kao, Z.-K.; Hung, Y.-H.; Liao, Y.-C. *J. Mater. Chem.* **2011**, *21*, 18799−18803.
(20) Zhang, H.; Xie, A.; Shen, Y.; Qiu, L.; Tian, X. *Phys. Chem. Chem. Phys.* **2012**, *14*, 12757−12763.
(21) Mionic, M.; Pataky, K.; Gaal, R.; Magrez, A.; Brugger, J.; Forro, L. *J. Mater. Chem.* **2012**, *22*, 14030−14034.
(22) Yoon, B.; Shin, H.; Yarimaga, O.; Ham, D.-Y.; Kim, J.; Park, I. S.; Kim, J.-M. *J. Mater. Chem.* **2012**, *22*, 8680−8686.
(23) Delaney, J. L.; Hogan, C. F.; Tian, J.; Shen, W. *Anal. Chem.* **2011**, *83*, 1300−1306.
(24) Jang, J.; Ha, J.; Cho, J. *Adv. Mater.* **2007**, *19*, 1772−1775.
(25) Yoon, B.; Lee, S.; Kim, J.-M. *Chem. Soc. Rev.* **2009**, *38*, 1958−1968.
(26) Sun, X.; Chen, T.; Huang, S.; Li, L.; Peng, H. *Chem. Soc. Rev.* **2010**, *39*, 4244−4257.
(27) Chen, X.; Zhou, G.; Peng, X.; Yoon, J. *Chem. Soc. Rev.* **2012**, *41*, 4610−4630.
(28) Lee, S. B.; Koepsel, R.; Stolz, D. B.; Warriner, H. E.; Russell, A. J. *J. Am. Chem. Soc.* **2004**, *126*, 13400−13405.
(29) Bai, F.; Sun, Z.; Lu, P.; Fan, H. *J. Mater. Chem.* **2012**, *22*, 14839−14842.
(30) Yarimaga, O.; Jaworski, J.; Yoon, B.; Kim, J.-M. *Chem. Commun.* **2012**, *48*, 2469−2485.
(31) Chance, R. R.; Baughman, R. H.; Muller, H.; Eckhardt, C. J. *J. Chem. Phys.* **1977**, *67*, 3616−3618.
(32) Dei, S.; Shimogaki, T.; Matsumoto, A. *Macromolecules* **2008**, *41*, 6055−6065.
(33) Ahn, D. J.; Lee, S.; Kim, J.-M. *Adv. Funct. Mater.* **2009**, *19*, 1483−1496.
(34) Patlolla, A.; Zunino, J., III; Frenkel, A. I.; Iqbal, Z. *J. Mater. Chem.* **2012**, *22*, 7028−7035.
(35) Charych, D.; Nagy, J.; Spevak, W.; Bednarski, M. *Science* **1993**, *261*, 585−588.
(36) Chen, X.; Kang, S.; Kim, M. J.; Kim, J.; Kim, Y. S.; Kim, H.; Chi, B.; Kim, S.-J.; Lee, J. Y.; Yoon, J. *Angew. Chem., Int. Ed.* **2010**, *49*, 1422−1425.
(37) Lee, J.; Jun, H.; Kim, J. *Adv. Mater.* **2009**, *21*, 3674−3677.
(38) Jung, Y. K.; Kim, T. W.; Park, H. G.; Soh, H. T. *Adv. Funct. Mater.* **2010**, *20*, 3092−3097.
(39) Kwon, I. K.; Song, M. S.; Won, S. H.; Choi, S. P.; Kim, M.; Sim, S. J. *Small* **2012**, *8*, 209−213.
(40) Kim, K. M.; Oh, D. J.; Ahn, K. H. *Chem. Asian J.* **2011**, *6*, 122−127.
(41) Chen, X.; Li, L.; Sun, X.; Liu, Y.; Luo, B.; Wang, C.; Bao, Y.; Xu, H.; Peng, H. *Angew. Chem., Int. Ed.* **2011**, *50*, 5486−5489.
(42) Cheng, Q.; Stevens, R. C. *Langmuir* **1998**, *14*, 1974−1976.
(43) Jeon, H.; Lee, J.; Kim, M. H.; Yoon, J. *Macromol. Rapid Commun.* **2012**, *33*, 972−976.
(44) Carpick, R. W.; Sasaki, D. Y.; Burns, A. R. *Langmuir* **2000**, *16*, 1270−1278.
(45) Peng, H.; Sun, X.; Cai, F.; Chen, X.; Zhu, Y.; Liao, G.; Chen, D.; Li, Q.; Lu, Y.; Zhu, Y.; Jia, Q. *Nat. Nanotech.* **2009**, *4*, 738−741.
(46) Wu, S.; Shi, F.; Zhang, Q.; Bubeck, C. *Macromolecules* **2009**, *42*, 4110−4117.

(47) Yoon, J.; Jung, Y.-S.; Kim, J.-M. *Adv. Funct. Mater.* **2009**, *19*, 209−214.
(48) Yoon, B.; Ham, D.-Y.; Yarimaga, O.; An, H.; Lee, C. W.; Kim, J.-M. *Adv. Mater.* **2011**, *23*, 5492−5497.
(49) Chebotareva, N.; Bomans, P. H. H.; Frederik, P. M.; Sommerdijk, N. A. J. M.; Sijbesma, R. P. *Chem. Commun.* **2005**, 4967−4969.
(50) Nasr, G.; Macron, T.; Gilles, A.; Petit, E.; Barboiu, M. *Chem. Commun.* **2012**, *48*, 7398−7400.
(51) Dautel, O. J.; Robitzer, M.; Lère-Porte, J.-P.; Serein-Spirau, F.; Moreau, J. J. E. *J. Am. Chem. Soc.* **2006**, *128*, 16213−16223.
(52) Koevoets, R. A.; Karthikeyan, S.; Magusin, P. C. M. M.; Meijer, E. W.; Sijbesma, R. P. *Macromolecules* **2009**, *42*, 2609−2617.
(53) Riggs-Sauthier, J.; Zhang, W.; Viegas, T. X.; Bentley, M. D. 2010, U.S. Patent 20100152201.
(54) Kim, J.; Lee, C.; Yoo, H.; Kim, J.-M. *Macromol. Res.* **2009**, *17*, 441−444.
(55) Coleman, M. M.; Sobkowiak, M.; Pehlert, G. J.; Painter, P. C.; Iqbal, T. *Macromol. Chem. Phys.* **1997**, *198*, 117−136.
(56) Giorgetti, E.; Muniz-Miranda, M.; Margheri, G.; Giusti, A.; Sottini, S.; Alloisio, M.; Cuniberti, C.; Dellepiane, G. *Langmuir* **2006**, *22*, 1129−1134.
(57) Kim, J.-M.; Lee, J.-S.; Choi, H.; Sohn, D.; Ahn, D. J. *Macromolecules* **2005**, *38*, 9366−9376.
(58) Pavlidis, T.; Swartz, J.; Wang, Y. P. *Computer* **1992**, *25*, 18−28.
(59) Kato, H.; Tan, K. T. *IEEE Pervas. Comput.* **2007**, *6*, 76−85.
(60) De Cremer, G.; Sels, B. F.; Hotta, J.-i.; Roeffaers, M. B. J.; Bartholomeeusen, E.; Coutiño-Gonzalez, E.; Valtchev, V.; De Vos, D. E.; Vosch, T.; Hofkens, J. *Adv. Mater.* **2010**, *22*, 957−960.
(61) Han, S.; Bae, H. J.; Kim, J.; Shin, S.; Choi, S.-E.; Lee, S. H.; Kwon, S.; Park, W. *Adv. Mater.* **2012**, *24*, 5924−5929.